

A simple model to quantitatively account for periodic outbreaks of the measles in the Dutch Bible Belt

Martin Bier^{1,2,a} and Bastiaan Brak³

¹ Department of Physics, East Carolina University, Greenville, NC 27858, USA

² M. Smoluchowski Institute of Physics, Jagiellonian University, ul. Lojasiewicza 11, 30-348 Kraków, Poland

³ School of Agriculture, Policy, and Development, The University of Reading, Whiteknights, P.O. Box 217, Reading, RG6 6AH, UK

Received 11 September 2014 / Received in final form 13 December 2014

Published online 22 April 2015

© The Author(s) 2015. This article is published with open access at Springerlink.com

Abstract. In the Netherlands there has been nationwide vaccination against the measles since 1976. However, in small clustered communities of orthodox Protestants there is widespread refusal of the vaccine. After 1976, three large outbreaks with about 3000 reported cases of the measles have occurred among these orthodox Protestants. The outbreaks appear to occur about every twelve years. We show how a simple Kermack-McKendrick-like model can quantitatively account for the periodic outbreaks. Approximate analytic formulae to connect the period, size, and outbreak duration are derived. With an enhanced model we take the latency period in account. We also expand the model to follow how different age groups are affected. Like other researchers using other methods, we conclude that large scale underreporting of the disease must occur.

1 Introduction

Upon hearing that vaccination against the measles is nowadays common in the entire developed world and in many developing countries, many people of the 50-and-older generation react with a statement like “Why? It’s just the measles . . .”. Indeed, until vaccination programs became common around 1970, almost every child would get the measles and, in Western countries, 99% recovered without lasting consequences. However, in 1980 the fraction of cases where complications did arise still resulted in an unacceptable 2 600 000 fatalities worldwide [1]. Vaccination programs have brought this number down to about 122 000 in 2012 [2]. The vaccine is cheap, safe, and effective, so vaccination programs make sense from a public health policy perspective.

In September 2010, the 53 member states of the WHO (World Health Organization) European Region agreed to commit to the ambitious goal to eliminate measles (and rubella) in Europe by 2015 [3]. Previously the deadline had been set for 2010. WHO defines measles elimination as “the absence of endemic measles transmission in a defined geographical area for more than 12 months in the presence of a well-performing surveillance system”.

The Dutch government implemented its nationwide vaccination program against the measles in 1976. The two-dose schedule was introduced in 1987. The national vaccine coverage of the first dose of the Measles-Mumps-Rubella (MMR1) vaccine has been fairly stable

at about 96% for the last 20 years. The national vaccine coverage for MMR2 is a bit lower, at 92% (Tab. 3b in [4]). Yet, as of June 2013, there are 30 municipalities in the Netherlands with less than 90% coverage for the MMR1 vaccine, in one case even lower than 60% [4]. The explanation for this reduced vaccination coverage is a geographic clustering – commonly referred to as “the Bible Belt”¹, a strip that runs from the south-west to the north-east of the country (Fig. 1) – of orthodox Protestants who refuse vaccination due to their interpretation of divine providence [5]. Recently the orthodox Protestant community has been estimated at 250 000 people [6,7]. The vaccination coverage within this community has been estimated to be at least 60% [8].

Nevertheless, in each of the three large measles outbreaks in the Netherlands over the last thirty years, orthodox Protestants, refusing vaccination on religious grounds, made up the majority of unvaccinated measles cases for which information was available (see Tab. 1).

There have been instances where an outbreak of an infectious disease followed after an isolated “virgin” population incidentally (re)encountered the agent of a disease [9]. In this context the 1846 outbreak of the measles on the Faroe Islands is famous [10]. In the Dutch Bible Belt, however, there have now been three large outbreaks (>1500 cases) of comparable magnitude that each lasted

¹ see Wikipedia, Bible Belt (Netherlands) (2014), http://en.wikipedia.org/wiki/Dutch_bible_belt [Accessed 01 June 2014]

^a e-mail: bierm@ecu.edu

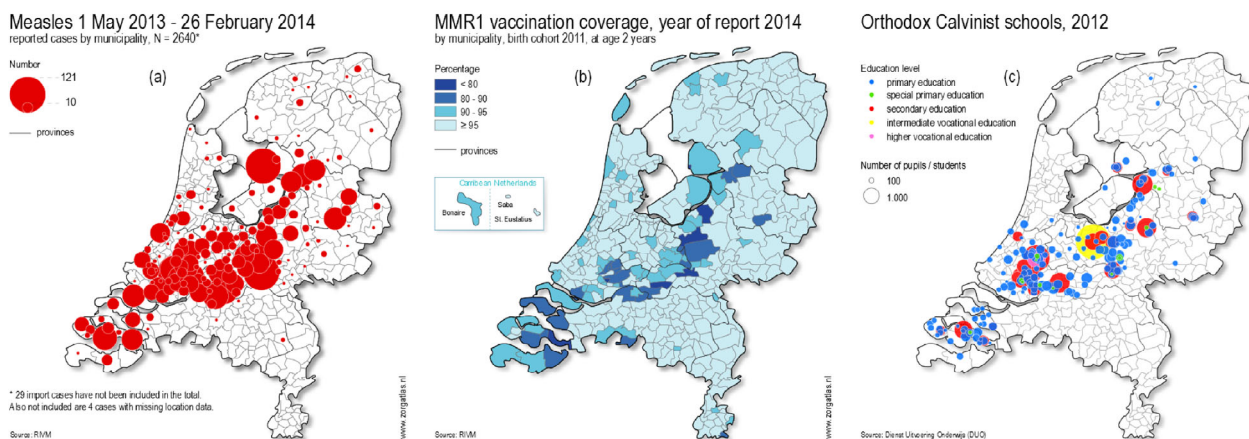


Fig. 1. The 2013/2014 outbreak of the measles in the Dutch Bible Belt. In (a) the area of each circle corresponds to the number of cases. (b) The percentage of children who are vaccinated before the age of 2. The darkest blue corresponds to a vaccination coverage of less than 80%. (c) The locations of the orthodox Protestant schools. Blue circles correspond to primary schools. Red circles correspond to secondary schools. The circle's area corresponds to the number of students in the school. These data-maps are produced by the Dutch National Institute for Public Health and the Environment (RIVM) and are available in the public domain (see footnote 6). They are reprinted with permission.

Table 1. The demographics for the three large measles outbreaks (>1000 cases) in the Netherlands.

	1987–1988	1999–2000	2013–2014 ¹
Reported cases	1666	3292	2744
Unvaccinated	1499	3092	2552
(% of reported cases)	(90)	(94)	(93)
Unvaccinated on Religious Grounds	966	2657	n/a
(% of reported cases)	(64)	(86) ²	(92) ³
<1 year old	34	195	71
(% of reported cases)	(2)	(6) ⁴	(3)
1–4 years old	540	985	438
(% of reported cases)	(32)	(30) ⁵	(16)
5–9 years old	640	1456	819
(% of reported cases)	(38)	(44)	(30)
10–14 years old	310	452	868
(% of reported cases)	(19)	(14)	(32)
15–19 years old	113	103	294
(% of reported cases)	(7)	(3)	(11)
≥20 years old	24	95	254
(% of reported cases)	(1)	(3)	(9)
Sources	Ref. [41]	Ref. [42]	Ref. [15], WHO ⁶

¹ Figures represent the period from May 2013 to April 2014. ² Individuals ≥ 15 months of age only. ³ As per February 12, 2014, when the number of reported cases stood at 2624. ⁴ Actual age bin: 14 months. ⁵ Actual age bin: 15 months to 4 years. ⁶ World Health Organization, Centralized Information System for Infectious Diseases (CISID) (2014), <http://data.euro.who.int/cisid/> [Accessed 24 July 2014].

about a year and came about 12 years apart (see Fig. 2 and Tab. 1). The first outbreak also came twelve years after vaccination started. The pattern suggests an underlying deterministic mechanism. The Netherlands is a densely populated country and because of ample and fast international travel, almost incessant “visits” of the measles virus are inevitable. The fact that sporadic measles cases still occur in between the major outbreaks is an illustration of this. It appears that, after a major outbreak, it takes the orthodox Protestant population about twelve years to

again accumulate sufficiently many susceptibles for a new major outbreak. It is the goal of this work to identify this deterministic mechanism and to quantitatively account for the observed oscillation.

It is precisely because of the self-imposed segregation that orthodox Protestants, unlike most other vaccine-refusing parents, do not benefit from herd immunity [11] and that large outbreaks can develop. The geographic and socio-demographic clustering of non-vaccinating orthodox Protestants has been recognized as the single largest

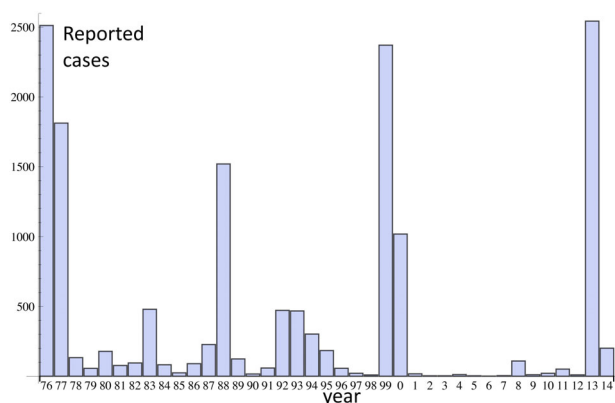


Fig. 2. The annual number of reported cases of the measles in the Netherlands in the period 1976–2014. Data are from the Dutch National Institute for Public Health and the Environment (see World Health Organization, Centralized Information System for Infectious Diseases (CISID) (2014), <http://data.euro.who.int/cisid/> [Accessed 24 July 2014]).

barrier to achieving the goal of eliminating measles in the Netherlands². In addition, outbreaks of vaccine-preventable diseases amongst orthodox Protestants in the Netherlands have clear repercussions abroad. Three measles outbreaks in Canada have been traced back to the 2013–2014 epidemic in the Netherlands³. In fact there is a long history of outbreaks of vaccine-preventable diseases such as poliomyelitis, mumps and rubella among Dutch orthodox Protestants spreading to Canada [12].

Schools play a crucial role in the transmission chain of measles [13,14]. The dip in the number of reported measles cases that is often visible during school holidays is a clear sign of this (see, for instance, Refs. [15,16]). It is in the schools that infectious, but as yet asymptomatic, and susceptible pupils spend a lot of time together and with measles transmission being airborne, contact rates will be high. With the penultimate measles outbreak in the orthodox Protestant community more than 12 years ago and the primary schools thus harboring many susceptibles, orthodox Protestant primary schools in particular can therefore arguably be seen as the driver of the 2013/2014 outbreak. Indeed, the first reports of measles cases in the 1999/2000 and 2013/2014 outbreaks came from orthodox Protestant schools [17]. In studying the dynamics of the epidemic, we therefore focus on the population in orthodox Protestant schools.

Religious denominations in the Netherlands can set up their own schools and can acquire public funding for these schools if a set of quality criteria is met⁴. There

² European Centre for Disease Prevention and Control (ECDC), National plan for measles elimination in the Netherlands (1999), <http://bit.ly/1bjWhHs> [Accessed 25 July 2014].

³ European Centre for Disease Prevention and Control (ECDC), Surveillance report – Measles and rubella monitoring (2014), <http://bit.ly/1xmpR91>. [Accessed 02 June 2014].

⁴ Ministry of Education, Culture, and Science, The Dutch Inspectorate of Education (2014), <http://www.onderwijsinspectie.nl/english> [Accessed 25 July 2014].

are about 180 orthodox Protestant primary schools⁵ and seven institutions for orthodox Protestant secondary education. The orthodox Protestant schools may differ in the details of their admissions policy, but it is common to admit only children from orthodox Protestant parents or to, at least, limit the admission of children from outside the orthodox Protestant community to a small percentage. No data are available on the percentage of “dissident” students across orthodox Protestant schools. But there is an ongoing debate in the orthodox Protestant press about this admissions policy and it appears that the schools that do admit “dissident” students, generally put their limit at 5 or 10 percent. So the fraction of students from outside the orthodox Protestant community is unlikely to be larger than 10%. According to open-source data from the Dutch Ministry of Education, Culture and Science, total enrollment in orthodox Protestant primary schools in 2010, 2011, 2012 and 2013 fluctuated around 39 000 pupils⁵. In the Netherlands primary schools cover eight years and students attend from age 4 to age 12. As mentioned before, the percentage of the orthodox Protestant community that does not vaccinate is estimated to be (at most) 40% [8]. Accounting for the vaccination coverage, the fact that the last major measles outbreak among orthodox Protestants was more than 12 years ago and assuming that on average 5% of pupils enrolled at orthodox Protestant primary schools comprise vaccinated children from outside the orthodox Protestant community, we can estimate that the population of susceptibles at the primary school level comprises about 15 000 pupils. Further assuming that these 15 000 pupils are equally distributed over all 8 grades, we infer that annually 1900 leave the population and 1900 new susceptible pupils enter. For our mathematical model this is the annual “supply” of new susceptibles and it is an important parameter. Again we mention that this 1900 is the upper limit that corresponds to the maximal 40% that does not vaccinate.

It is worth noting that the orthodox Protestant constitute only a minority among the non-vaccinated. Previously, this was estimated to be 15% [17], but the authors did not elaborate on how they arrived at this. With the same open source data that we used in the last paragraph, we estimate it as follows: first, we take the number of children attending orthodox Protestant “reformatorisch” primary schools and the number of all children attending primary schools. Next, we correct the number of children attending orthodox Protestant primary schools for vaccinated non-Protestant children attending these schools (1–10%). Finally, by estimating a plausible range of MMR1 vaccination coverage among orthodox Protestants (60%–70%) and among primary school pupils nationally (~97%; MMR1 vaccination coverage is 96% for 2 year olds and rises to 97.5% for 10-year olds), it can be estimated that the proportion of pupils

⁵ Ministry of Education, Culture, and Science, Passend Onderwijs, Kengetallen primair onderwijs (PO0001 Landelijk reformatorisch) (2014), <http://passendonderwijs.nl/wp-content/uploads/2013/04/PO0001-Landelijk-Reformatorisch1.xls>

not having received vaccination based on religious beliefs constitutes between 23 and 33 percent of the total non-vaccinated.

Understanding the size and timing of outbreaks of vaccine-preventable diseases is paramount when assessing the risk of future outbreaks [18]. Epidemic models provide an essential tool in this. One of the earliest, classic approaches is the compartmental SIR model proposed by Kermack and McKendrick [19]. In SIR models people are either “Susceptible”, “Infected”, or “Removed”. “Removed” individuals have died or become immune to infection. In either case, the “Removed” no longer participate in the dynamics of the disease. One of the central outcomes of the model of Kermack and McKendrick is that the number of susceptibles in a population must be above a certain threshold for an epidemic to occur [11,19,20]. Data on real epidemics reveal ample illustration of the reality of such a threshold [18]. In the research described in this paper, we slightly modify the original model of Kermack and McKendrick to apply to the long-term dynamics of measles outbreaks in the Netherlands. In Section 2 a simple model is presented to reproduce the sharply peaked periodic outbreaks. In Section 3 analytic formulae to approximate the period and the magnitude of the outbreak are derived. In Section 4 more characteristics of the disease are taken into account. The model is extended and fine-tuned to reproduce the observed age distributions and the shift of the patients’ age distribution from one outburst to the next (Tab. 1). Section 5 is the results and discussion section.

Primary and secondary schools as well as medical professionals in most European countries are required to report measles cases to the authorities. However, for one municipality in the Netherlands it was found that the number of reported cases during the 1999/2000 measles epidemic constituted just 9% of all measles cases diagnosed retrospectively [21]. Similar figures have been reported in relation to outbreaks in Germany [22] and France [23]. The results of our modeling will provide an independent affirmation of the large scale underreporting.

2 A basic model

Children of the orthodox Protestant community commonly commute long distances in order to go to orthodox Protestant schools. The “mixing” in these schools homogenizes the orthodox Protestant population to a large extent with respect to the disease. We thus treat the orthodox Protestant population as one reservoir and use the “continuously stirred tank reactor”-approach of chemical kinetics. This means that in setting up a model, we use ordinary differential equations and time will be the only independent variable. An animation on a Dutch-government website⁶ shows the progress of the 2013/2014 outbreak in time. No clear cross-country prop-

agation is apparent in this animation. So the continuously stirred tank reactor is a reasonable approach.

We let $S(t)$ be the number of susceptibles and let $I(t)$ be the number of infected. The following simple autonomous system can reproduce the periodic outbursts. The model resembles the well-known model of Kermack and McKendrick that was first proposed in 1927 [19],

$$\dot{S} = A - \alpha SI \quad \text{and} \quad \dot{I} = \alpha SI - \beta I. \quad (1)$$

Here the dot represents differentiation w.r.t. time, i.e. $\dot{\bullet} \equiv d/dt$. We take a day as our unit of time. In the introduction we found that the population of susceptibles increases at a rate of at most 1900 per year. This means an upper limit of $A \approx 5$ for the daily increase. A person that is infected with the measles is contagious and relatively free of symptoms for about four to nine days before the characteristic rash starts and the student stops going to school. We thus take $\beta \approx 0.15$ for the rate at which infected are removed. The parameter α is the contact rate. This parameter represents the fraction of the susceptibles that an average infective successfully exposes per day. It depends not only on the infectiousness of the disease, but also on social organization. It may vary seasonally. We use $\alpha \approx 5 \times 10^{-6}$, which is similar to values used by Yorke and London to explain two-year periodic measles outbursts among non-vaccinated people in New York City in the 1960s [24].

Setting the left hand sides of equations (1) equal to zero, we find the fixed point in the (S, I) -plane:

$$(S_0, I_0) = \left(\frac{\beta}{\alpha}, \frac{A}{\beta} \right). \quad (2)$$

Next, a linear analysis will reveal the behavior of equations (1) in the vicinity of the fixed point. To that end, we substitute $S(t) = S_0 + \delta(t)$ and $I(t) = I_0 + \varepsilon(t)$. We neglect the quadratic terms in δ and ε and then solve the resulting system of linear differential equations for $(\delta(t), \varepsilon(t))$ [20]. For the solution of the eigenvalue equations, we get

$$\lambda_{1,2} = -\frac{A\alpha}{2\beta} \pm \frac{1}{2} \sqrt{\frac{A\alpha(A\alpha - 4\beta^2)}{\beta^2}}. \quad (3)$$

For a damped oscillation, i.e. the fixed point being a stable spiral, we need the term under the square root to be negative. For our parameter values we indeed have $4\beta^2 \gg A\alpha$. We thus get $\omega \approx \sqrt{\alpha A}$ for the angular velocity in the (S, I) -phase plane and, consequently, $T = 2\pi/\omega = 2\pi/\sqrt{\alpha A}$ for the period. The real part of $\lambda_{1,2}$ represents the damping coefficient and it determines how fast the amplitude of the oscillation gets smaller. For the parameter values that we use, the damping coefficient is between one and two orders of magnitude smaller than ω . So the damping is slow relative to the oscillation and we are looking at a system with a very recognizable periodicity.

There was, of course, no change in the infectiousness α and the recovery rate β when nationwide vaccination in the Netherlands started. But there was a dramatic change

⁶ Dutch National Institute for Public Health and the Environment (RIVM), Mazelen in de Bible Belt (2014), <http://bit.ly/19F8t53> [Accessed 02 August 2014].

in the daily supply of new susceptibles A . Before vaccination it was orders of magnitude larger and, as a result, λ_1 and λ_2 (cf. Eq. (3)) were negative numbers. Such $\lambda_1, \lambda_2 < 0$ leads to a phase plane structure with a rapid non-oscillatory relaxation to the fixed point. Before nationwide vaccination, the number of infected people in the Dutch population stayed constant at a level $I_0 = A/\beta$.

When nationwide vaccination started, the dynamical system equation (1) was left in a state far from a new fixed point – a fixed point that, because of the new small A , now had complex valued λ_1 and λ_2 (cf. Eq. (3)) and a resulting stable spiral around it.

We saw earlier that post-1976 we have at most $A \approx 5$. As was mentioned before, the eight grades in Dutch primary schools cover ages 4 to 12. With the aforementioned 15 000 children in the orthodox Protestant schools, we have $15\,000/8 \approx 1900$ children per grade. Because in the pre-vaccination era, children get the measles on average at age 10, there will be about 11 000 susceptibles in the orthodox Protestant schools in 1977. To these susceptibles we have to add the ones in the zero-to-four age group, i.e. four times the number of children per grade. This reasoning leads us to the estimate of $S(0) \approx 20\,000$ for the 1977 situation. For the number of infected in the orthodox Protestant community at $t = 0$, we take the pre-1977 constant level $I_0 = A/\beta$. With at most $A \approx 5$ for the orthodox Protestant community, we have $I(0) \approx 20$. But it turns out that the final outcome is not sensitive to the value of $I(0)$. Figure 3 shows the result of a simulation. The 12-year periodicity with sharp peaks is reproduced in the simulation.

Even though no general solution is available, equations (1) are sufficiently simple that approximations can be derived. Next we will perform an analysis that will lead to formulae that connect the “inter-outbreak” interval, the duration of an outbreak, the number of infections and the parameters A , α , and β .

3 Approximating the outbreak’s size, period, and duration

The linear approximation that gives rise to equation (3) describes damped harmonic oscillations. It is obvious that the oscillations that we see in Figure 3 are not harmonic. They are too far away from the fixed point for the linear approximation to be valid. The oscillation that we see can be separated out into two clearly identifiable stages: (1) the inter-outbreak interval and (2) the outbreak. The function $S(t)$ looks like a sawtooth wave with a small damping. During the inter-outbreak interval, the number of susceptibles is growing linearly while the number of infected remains close to zero, i.e. $dS/dt \approx A$ and $I \approx 0$. During the outbreak, the absolute value of dS/dt is much larger than A . The outbreak dynamics is thus well approximated by just:

$$\dot{S} \approx -\alpha SI \quad \text{and} \quad \dot{I} \approx \alpha SI - \beta I. \quad (4)$$

With equations (4) we are back at the traditional SIR model of Kermack and McKendrick. Equations (4) also

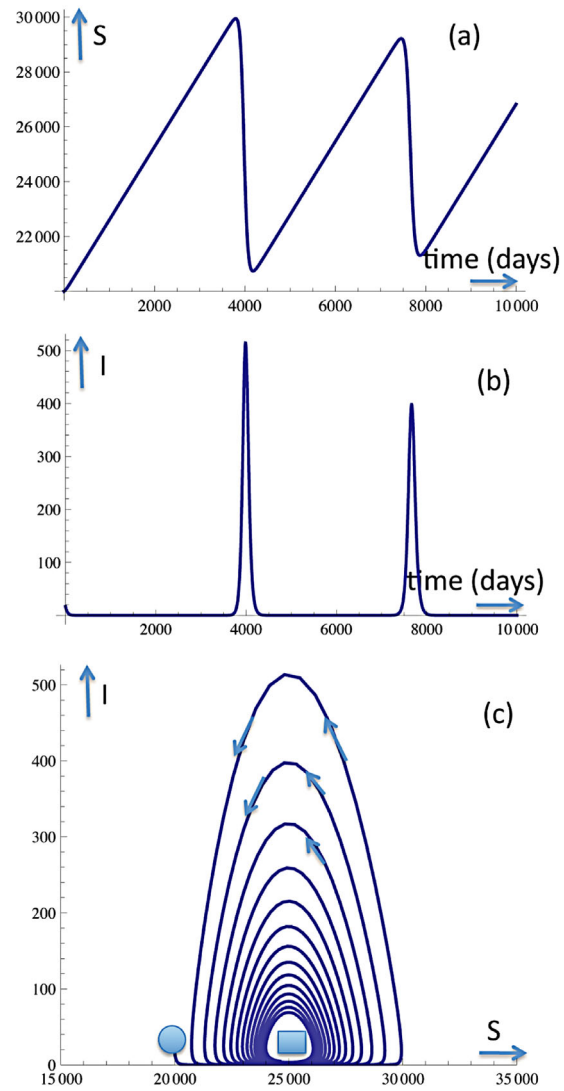


Fig. 3. A numerical simulation of equations (1) using *Mathematica*. The initial conditions, $S(0) = 20\,000$ and $I(0) = 17$, mimic the 1977 situation within the orthodox Protestant community after the rest of the nation was vaccinated. We take $A = 2.7$ for the daily influx of new susceptibles, $\beta = 0.12$ for the daily removal rate of infected, and $\alpha = 4.8 \times 10^{-6}$ for the contact rate. Plotted are (a) the number of susceptibles S and (b) the number of infected I as functions of time. Panel (c) shows more than 100 years of the time evolution of the system in the (S, I) -phase plane. The circle and the square indicate the initial condition and the stable fixed point, respectively.

constitute a special case of the well-known Lotka-Volterra system [11,20]. The Lotka-Volterra equations describe the dynamics in a predator-prey system. With $x(t)$ being the number of prey and $y(t)$ being the number of predators, the Lotka-Volterra system is: $\dot{x} = ax - xy$ and $\dot{y} = -by + xy$. The Lotka-Volterra system has no general analytic solution with two free constants to match initial conditions, but one integral, $\ln(x^b y^a) = x + y + C$, where C is one constant determined by initial conditions, is readily derived [20]. In our case we have $a = 0$.

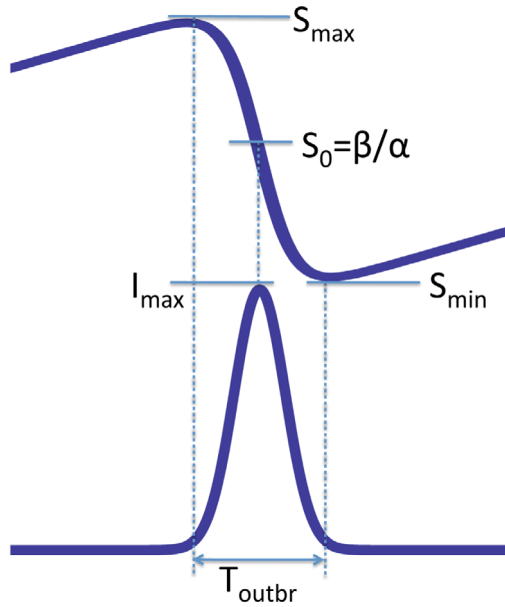


Fig. 4. Schematic representation of the outbreak part of the dynamics as seen in Figure 3. The number of susceptibles (top) is seen to drop rapidly from S_{\max} to S_{\min} in an almost straight line. The midpoint, $S_0 = \beta/\alpha$, corresponds to the time at which the number of infected (bottom) reaches its maximum. By taking the decrease of S to be linear, simple expressions to connect the relevant quantities can be derived.

For equations (4) the integral ultimately takes the form $I = (\beta/\alpha) \ln S - S + C$, where C is again a free constant.

Figures 3 and 4 show how the number of infected $I(t)$ reaches its maximum I_{\max} at the moment that $S(t)$ goes through its average (which is the fixed point value $S_0 = \beta/\alpha$). We can obtain the value of the constant of integration C by substituting $(S, I) = (S_0, I_{\max})$. We thus find

$$I = I_{\max} + S_0 \left[\ln \left(\frac{S}{S_0} \right) + 1 \right] - S. \quad (5)$$

Figure 4 shows that at $S = S_{\max}$ and $S = S_{\min}$, we have $I \approx 0$. Substituting $I = 0$ in equation (5) we find an equation for S :

$$\frac{I_{\max}}{S_0} = \frac{S}{S_0} - \ln \left(\frac{S}{S_0} \right) - 1. \quad (6)$$

The two solutions for S are S_{\min} and S_{\max} . In Figure 3 we see that S stays close enough to S_0 to warrant taking $S/S_0 = 1 + \epsilon$ and the second order Taylor approximation $\ln(1 + \epsilon) \approx \epsilon - \epsilon^2/2$. We are then led to the simple relation $I_{\max}/S_0 \approx \epsilon^2/2$ and, consequently,

$$S_{\max} \approx S_0 \left(1 + \sqrt{\frac{2I_{\max}}{S_0}} \right), \quad S_{\min} \approx S_0 \left(1 - \sqrt{\frac{2I_{\max}}{S_0}} \right). \quad (7)$$

For the number of people infected during an outbreak we thus have

$$S_{\max} - S_{\min} \approx 2\sqrt{2I_{\max}S_0}. \quad (8)$$

During the inter-outbreak interval this is how much S has to grow through the influx A . As the duration of the outbreak is much smaller than the inter-outbreak interval, we can take the inter-outbreak interval as the period. For the period T_{per} we then have the approximation:

$$T_{per} \approx \frac{S_{\max} - S_{\min}}{A} \approx \frac{2}{A} \sqrt{2I_{\max}S_0}. \quad (9)$$

We can also derive an approximate value for the duration of the outbreak, T_{outbr} . Figures 3 and 4 show an almost linear decrease in time from S_{\max} to S_{\min} . The slope at the midpoint (S_0, I_{\max}) is a good approximation for the almost constant rate at which infections occur during the outbreak. With $|\dot{S}|_{outbr} \approx \alpha S_0 I_{\max}$ we have

$$T_{outbr} \approx \frac{S_{\max} - S_{\min}}{|\dot{S}|_{outbr}} \approx \frac{2}{\alpha} \sqrt{\frac{2}{S_0 I_{\max}}}. \quad (10)$$

Figure 3 shows the time evolution that equations (1) predict. To generate Figure 3, we took the parameter values $A = 2.7$, $\beta = 0.12$, and $\alpha = 4.8 \times 10^{-6}$. We motivated these values earlier. These values lead to $S_0 = \beta/\alpha = 25\,000$. The depicted time evolution of “ S ” and “ I ” indeed displays the sharply peaked outbreaks that occur in real life about every ten to twelve years.

In Figure 3 we see that the first outbreak has its peak at $I_{\max} \approx 500$. Substituting this into equations (9) and (10), we find $T_{per} \approx 3700$ days and $T_{outbr} \approx 170$ days. The period T_{per} is indeed close to the observed twelve years, but the outbreak time T_{outbr} appears to underestimate the real outbreak-time by about a factor two. This is because the model does not take the latency period into account. In our model an infected person is immediately contagious. In actual reality a person is non-contagious and without symptoms for a week to ten days after infection. It can be readily intuited that this latency period extends the time that the outbreak lasts. Modifying equations (1) to take the latency period into account is straightforward. The result is a system of so-called delay differential equations. Such equations are notoriously hard to analyze. In Section 4.1 we will model the latency period through the addition of one extra linear equation to equations (1). It is indeed found that the only major effect of the latency period is an extension of the outbreak time.

Entering the values for I_{\max} and S_0 into equation (8), we find that about 10000 people are infected during the outbreak. The fraction of susceptibles that gets infected during an outbreak can also be evaluated in another way. The analysis of equations (4) often involves the number $R_0 = S(0)\alpha/\beta$, which represents the number of susceptibles infected by one infected person at the beginning ($t = 0$) of the outbreak. For the case depicted in Figure 3 we see that $R_0 \approx 1.2$ when the first outbreak begins. Manipulating equations (4), the following equation for the fraction of susceptibles s that does not get infected during an outbreak can be derived: $s = \exp[R_0(s - 1)]$ (see e.g. [20], Sect. 19.1). Solving this equation numerically for $R_0 \approx 1.2$, we find $s \approx 0.69$. So only about one third of the susceptibles is infected in the course of the outbreak. This is also what Figure 3a shows.

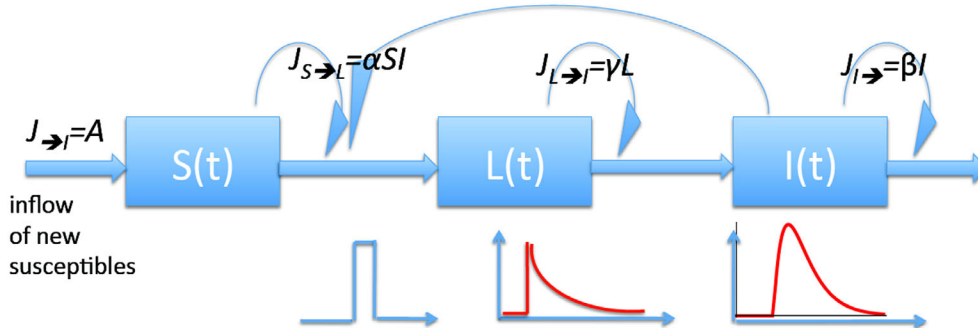


Fig. 5. Depiction of equations (13) as a flow through three different reservoirs, S , L , and I . The thick arrows and the J 's depict the flows from one reservoir to the next. The thin arrows indicate how the quantities in the reservoirs feed back on the flows. On the bottom it is shown what happens when a delta function like pulse moves from S to L to I . There will be a step function like increase in L , followed by an exponential relaxation, i.e., $L(t) \propto \exp[-\gamma t]$ and therefore $J_{L \rightarrow I} \propto \exp[-\gamma t]$. In I we finally get a rise and fall that follows a double exponential $I(t) \propto \exp[-\gamma t] - \exp[-\beta t]$.

This result is remarkable in two ways. Each of the three outbreaks involved about 3000 reported cases. If the model is correct and about 10 000 of 30 000 susceptibles are infected in the course of an outbreak, then this would imply that there is an underreporting by about a factor three! We see the underreporting factor of three not just in the *total* number of reported cases. Figure 3 shows that the number of infected at one and the same time is maximally $I_{\max} \approx 500$. Figure 1 in reference [15] is a histogram that gives the number of reported cases per week during the 2013/2014 outbreak. It shows a maximum of 180 reported cases in a week. The I in the model should correspond to the number of new cases per week as the “ I -status” lasts about $1/\beta \approx 7$ days. The 500 in the model is indeed about 3 times the 180 in the histogram. In the results and discussion section we will come back to the underreporting issue. Furthermore, if such a large fraction of the susceptibles does *not* get infected in the outbreak, then the number of older susceptibles must have been growing since 1976 and make up for an ever larger fraction of the infected with every subsequent outbreak since the first one in 1988. We will check on this model prediction in Section 4.2 and we will discuss its public health consequences in the results and discussion section.

4 Enhanced models

4.1 The effect of the latency period

As was mentioned before, the measles has a latency period, Δt , of 7 to 10 days. This means that the increase of the number of infectious people at time t equals the number of infections at time $t - \Delta t$. Taking this delay into account, equations (1) become

$$\dot{S}(t) = A - \alpha S(t)I(t)$$

and

$$\dot{I}(t) = \alpha S(t - \Delta t)I(t - \Delta t) - \beta I(t). \quad (11)$$

The second equation of (11) can be rewritten as:

$$\dot{I}(t + \Delta t) = \alpha S(t)I(t) - \beta I(t + \Delta t). \quad (12)$$

In Figure 3 it can be seen that $S(t)$ and $I(t)$ change little in the course of just 10 days. We thus take a first order Taylor approximation, i.e. $I(t + \Delta t) = I(t) + (\Delta t)\dot{I}(t)$ and $\dot{I}(t + \Delta t) = \dot{I}(t) + (\Delta t)\ddot{I}(t)$. Substituting this in (12) and taking $\dot{I} + \beta I = \gamma L$, where $\gamma = 1/\Delta t$, we derive:

$$\begin{aligned} \dot{S}(t) &= A - \alpha S(t)I(t) \\ \dot{L}(t) &= \alpha S(t)I(t) - \gamma L(t) \\ \dot{I}(t) &= \gamma L(t) - \beta I(t). \end{aligned} \quad (13)$$

With equations (13) the delay has been removed and translated into an extra dimension of the system. The new dependent variable $L(t)$ represents the “latents”. After leaving the susceptibles, an individual now spends an average time $1/\gamma$ in the “latents” reservoir before it moves to the “infected” (see Fig. 5). The model depicted in Figure 5 is known in the literature as the SLIR model. Often the latents are called “exposed”. The same model is then called SEIR [25].

With Figure 5 it can be understood how the latency time $1/\gamma$ extends the duration of the outbreak time $T_{outbr.}$. Imagine a “sudden blip” that is passed on from S to L . A delta-function-like “blip” going from S to L results in a step-function-increase in L . This step-function-increase is next passed on to I with a relaxation time $1/\gamma$. It then moves out of I to leave the system with a relaxation time $1/\beta$. Solving the associated differential equations, one easily ascertains that the delta function “blip” that moved from S to L at $t = 0$ results in a signal in I that follows $I(t) \propto \exp[-\gamma t] - \exp[-\beta t]$. If reservoir L is not there or, equivalently, if $\gamma \rightarrow \infty$, then equations (1) are retrieved and the relaxation time out of I is just $1/\beta$. We can approximate the relaxation time out of reservoir I with $1/\gamma + 1/\beta$. This means that $(\gamma + \beta)/\gamma$ is the approximate factor by which the introduction of a latency time $1/\gamma$ widens the pulse.

If a chain of transmission of the measles involves N subsequent individuals, then going from equations (1) and Figure 3 to equations (13) leads to an extension of the duration of this chain. The duration of the chain will go from N/β to $N/\gamma + N/\beta$, i.e. an increase by the aforementioned

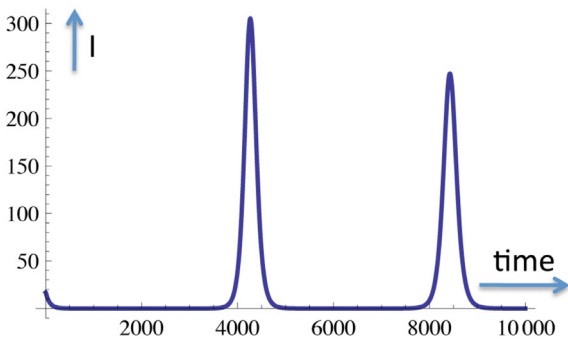


Fig. 6. The results of a simulation of equations (13). Initial conditions and parameter values are the same as those for Figure 3. In addition, we take $\gamma = 0.12$ to characterize the newly introduced latency (cf. Fig. 5). Depicted is the number infected as a function of time. Comparison with Figure 3b shows how the introduction of the latency state leads to wider peaks, i.e. a longer lasting outbreak time. The inter-outbreak period of 12 years remains unaffected.

factor $(\gamma + \beta)/\gamma$. The factor $(\gamma + \beta)/\gamma$ is therefore also expected to be the approximate factor by which the latency extends the T_{outbr} shown in Figure 4. The approximations of the previous section led to $T_{outbr} \approx 170$ days. With a latency period that is about equal to the infectiousness time (i.e. $1/\gamma = 1/\beta$), we then find that T_{outbr} gets about twice as long. Figure 6 depicts the results of a simulation of equations (13). As in Figure 3b, the number of infected is depicted as a function of time. Compared to Figure 3b, Figure 6 indeed shows a widening of the peaks by a factor of about two. Around a year is also the time that the real outbreaks are seen to last. Figure 6 furthermore shows how the inter-outbreak time of about twelve years is not affected when a latency period is introduced.

4.2 Separation into age groups

As can be seen in Table 1, for all of the three outbreaks 60% of reported measles cases involve school-age (5–14) children. The data of the 2013/2014 outbreak show that children in the 5–14 age group are about twice as likely to get infected as compared to children in the 0–4 and 15–19 age groups. Given the epidemiological dynamics of the disease, this is easily explained. When the previous outbreak occurred, the group that is older than 12 years of age was already present and the group that is older than 16 years of age was already present and even in school. The group that is younger than 5 years is, in large part, not going to school yet. As we stated before, it is the many close contacts between susceptibles and infected in orthodox Protestant schools that should be considered as the engine behind the epidemic. In the Discussion section of their article Yorke and London also conclude that the contact rate for the measles is “made” by children gathering in schools [24].

In a more detailed model, we subdivide the susceptibles into three groups: a population of 4 years of age and younger (S_1), a schoolgoing population of 5 to 14 years of age (S_2), and a population of 15 and older (S_3). We come

to the following dynamical system:

$$\begin{aligned} \dot{S}_1 &= A - \mu_1 S_1 - \alpha_1 S_1 I_2 & \dot{I}_1 &= \alpha_1 S_1 I_2 - \beta I_1 \\ \dot{S}_2 &= \mu_1 S_1 - \mu_2 S_2 - \alpha_2 S_2 I_2 & \dot{I}_2 &= \alpha_2 S_2 I_2 - \beta I_2 \\ \dot{S}_3 &= \mu_2 S_2 - \alpha_3 S_3 I_2 & \dot{I}_3 &= \alpha_3 S_3 I_2 - \beta I_3. \end{aligned} \quad (14)$$

Four years correspond to about 1500 days. However, for about the first half year of his or her life, a young child carries an immunity that it got from the mother. For our model this means that a susceptible is effectively born at the age of half a year. We thus take $\mu_1 = 1/1300$ as the rate at which susceptibles “flow” from S_1 to S_2 . We will take $\mu_2 = 1/3700$ (ten school years is 3700 days) as the rate of flow from S_2 to S_3 . The model neglects infections *within* S_1 and *within* S_3 . School-age children can infect their parents (S_3) and their younger siblings (S_1), but the parents and younger siblings do not infect anybody else. As most parents have already acquired immunity and as most infants stay at home, this is not an unreasonable assumption. If we took, for instance, toddler-to-toddler infections into account, it would add an $S_1 I_1$ product to the equations for \dot{S}_1 and \dot{I}_1 . Taking toddler-to-student infections into account would add an $S_2 I_1$ product to the equations for \dot{S}_2 and \dot{I}_2 . Each of these products would come with its own prefactor. These prefactors are hard to estimate. Our neglecting is justified by the fact that, as was mentioned before, the infections occurring in the orthodox Protestant schools are the “engine” of the epidemic. It is in these schools that the conditions for herd immunity are breached. The contact rate α is higher for infections within the school age population than for infections from the school age population to the other age groups.

The results of the simulation of equations (14) are depicted in Figure 7. For the indicated parameter values there are again sharply peaked outbreaks every twelve years (not shown). The simulation also reproduces how the different age groups are afflicted.

Table 1 and Figure 7 show how the fraction of patients in the 15+ category roughly doubles from one outbreak to the next. The reason for this can be easily intuited. In Figure 3 it can be seen that not all susceptibles are infected during an outbreak. Simulations of equations (14) show a steady increase in susceptibles in the 15+ category. Before vaccination everybody got the measles and the number of susceptible adults was effectively zero in 1977. After 1977, susceptible schoolchildren that did not get infected during an outbreak were susceptible adults during the next outbreak. We thus get correspondingly more victims in the 15+ category with every outbreak.

5 Results and discussion

Groundbreaking work on the mathematical epidemiology of the measles was done by Yorke and London in the 1970s [24]. They used a model similar to ours to explain biennial measles outbreaks among the non-vaccinated in New York City. They found that the seasonal variations

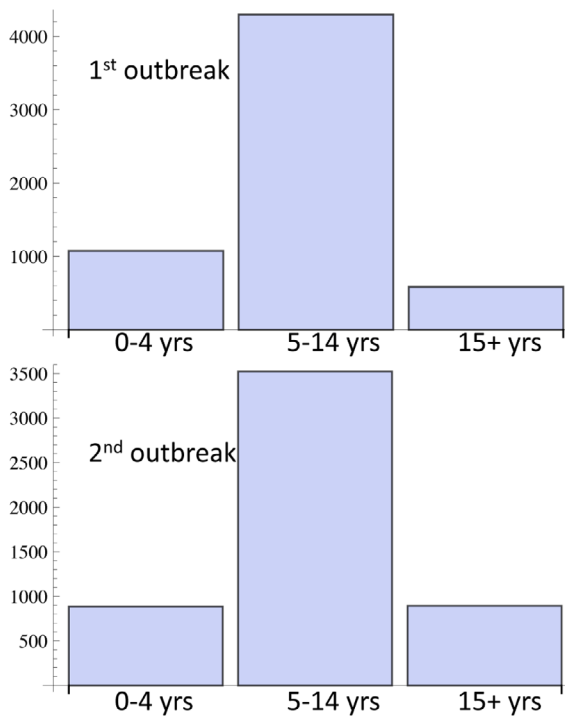


Fig. 7. The result of a simulation of equations (14). We took $S_1(0) = 6500$, $S_2(0) = 11000$, $S_3(0) = 1$, $I_1(0) = 1$, $I_2(0) = 10$, and $I_3(0) = 1$ as the initial condition describing the situation in 1977 after vaccination had begun. Parameter values are $A = 5$, $\mu_1 = 1/1300$, $\mu_2 = 1/3700$, and $\beta = 0.12$. Contact rates are different for the different age groups: $\alpha_1 = 5.0 \times 10^{-6}$, $\alpha_2 = 8.6 \times 10^{-6}$, and $\alpha_3 = 1.0 \times 10^{-6}$. Shown is the age structure of the population of victims in the first two outbreaks. It is apparent that the later outbreak has a larger fraction of patients in the 15+ category.

of the contact rate are essential for the oscillation to occur. The contact rate for their fit was up by a factor 2 in the winter when schools are in session and people spend more time in enclosed spaces. They found incubation time and latency time to be essential for the periodic pattern. In our case the inter-outbreak time is almost an order of magnitude larger than in the biennial case of Yorke and London. The latency time, the incubation time, and the seasonal variations of the contact rate will not affect our long inter-outbreak time. But, as we saw, the latency time will affect the peak width of our outbreaks. Other work on the periodic outbreaks of the measles also dealt with shorter periods and made use of seasonally changing contact rates [26,27]. Even chaotic behavior could occur in the ensuing dynamical systems. Our basic dynamical system, (Eq. (1)), and its enhancements are still way too simple to allow for anything like chaos. The underlying cause for the recurrent outbreaks in our model is found in the steady buildup of the number of schoolgoing susceptibles. After about 12 years of buildup, a threshold is crossed and the system is ready for a new chain reaction.

Interestingly, Yorke and London also concluded that there must be significant underreporting in the New York City case. They observed how the reported data were not

compatible with the fact that almost everybody got the measles before the age of 20. They estimated a factor 8 for the underreporting.

As was mentioned in Section 3, the Kermack-McKendrick theory leads to an equation for a threshold: $R = S\alpha/\beta$, where S represents the number of susceptibles. This R is the number of susceptibles that an average infective will infect. For $R > 1$ the number of infected will increase. For $R < 1$ the disease will die out. In a real world situation like ours it is often hard to apply the threshold theorem. This is mostly because the contact rate α is not sharply defined. Yorke and London already discussed the temporal variations. Figure 1 of reference [15] shows, for the 2013/2014 measles outbreak in the Dutch Bible Belt, the number of cases reported weekly and where these cases occurred. There is a clear summer-holiday dip. This is due to a smaller contact rate α when schools are not in session. But the contact rate α does not just vary in time. The continuously stirred tank reactor is a simplification. In Figure 1 of reference [15] we see that different schools are struck at different times. Schools in the south-eastern part of the Dutch Bible Belt (Gelderland-Zuid) were struck before the summer holidays. Schools in the western part (Rotterdam Rijnmond) were struck after the summer holidays. In other words, contact rates are high within a school, but for the transmission from one school district to another school district the α is lower and the threshold correspondingly higher. Smaller outbreaks that stay limited to one or just a few schools are therefore in principle possible. Figure 2 shows a small outbreak like that in 1983. In reference [28] it is described and explained how small scale outbreaks of the measles occur independently and randomly in different communities in England and Wales. That there is only the small outbreak of 1983 in our Dutch-Bible-Belt case indicates that the community-to-community contact rates within the Dutch Bible Belt are generally too high to allow for the limited, independent outbreaks of reference [28].

The outbreak in 1992/1993 [29] and the small outbreak in 2008 [30,31] that are apparent in Figure 2 are outbreaks that did not occur in the orthodox Protestant community. These outbreaks occurred in the anthroposophic community. The anthroposophists are a “spiritual” minority that also refuses vaccination against the measles [32,33]. They number less than the orthodox Protestants and they are also less clustered. But like the orthodox Protestants, they do operate a number of their own primary and secondary schools (see Ref. [34]). According to equation (10) the smaller contact rate and the smaller number of anthroposophists should lead to a longer outbreak time $T_{outbr.}$. This is indeed what we see in Figure 2: the 1992/1993 outbreak carries on into 1994 and 1995. The 2008 outbreak in the anthroposophist community stayed limited to only 99 cases. It was quickly contained and occurred mostly in just two cities [31].

In our simulations we see the number of infected go down to far below unity during the inter-outbreak intervals. In Figure 3b the number of infected, $I(t)$, actually reaches a value of $I = 2 \times 10^{-9}$ at about $t = 2000$. It is,

of course, highly unrealistic that the virus survives in a small fraction of a person and that a next outbreak can start from such a “small fraction of a person”. This problem has been encountered before in epidemic models and in predator-prey models [35]. In the context of predator-prey systems it has been called the “atto-fox problem” (atto = 10^{-18}). It needs to be realized that in the situation studied here, the virus is actually continuously around, even when nobody in the community is infected. Many times a year it is brought to the Dutch Bible Belt from the outside. However, as long as an infected individual infects on average less than one susceptible, any such introduction will *not* lead to an outbreak. In our simulations we actually found that the outbreak dynamics and the 12-year periodicity are rather insensitive to the initial value of the number of infected. Ultimately, it is the slow buildup of the number of susceptibles in the inter-outbreak intervals that matters much more for the dynamics. More realistic would be simulations with a small additive noise term in the expressions for \dot{I} and \dot{L} in equations (1), (13), and (14). But this would greatly take away from the simplicity of the model.

In our basic model we see that the number of infected never exceeds 500. Our numbers are small enough that just the stochastic nature of viral transmission can make for considerable variations from the average. A Master Equation approach [36] would give the probability $P(S, I, n+1)$ of S susceptibles and I infected on day $n+1$ as a function of $P(S, I, n)$. Such an approach should not just retrieve equations (1) for the averages, but it should also yield standard deviations.

The analysis of the nonlinear epidemic models with Master Equations and added noise is challenging, but elegant work has been done in that direction [37,38].

Equations (1) constitute a simple deterministic model without freely adjustable parameters. It is remarkable that such a basic model leads to such an accurate reproduction of the outbreak dynamics. Two results of our analysis are significant from a public health perspective.

Substantial field-research efforts have been done in order to come to a quantitative assessment of the underreporting of measles cases. Reporting is mandatory in the Netherlands, but in one low-vaccine-coverage municipality during the 1999/2000 outbreak, it was found that only about 30% of measles cases were presented to a medical professional and that medical professionals, in turn, reported only 30% of these cases to the authorities [21]. So just about 10% of cases were ultimately reported. In reference [23] the same estimate of 10% is arrived at for a measles outbreak in Southern France. In reference [22] the authors analyze data associated with a recent measles outbreak in the German state of North Rhine-Westphalia. The authors compare the number of cases that physicians have reported to the authorities with the number of cases that they derive from billing data of health insurers. They found negligible discrepancy during outbreaks, but more substantial discrepancy for times when no outbreak is going on. However, the method of these authors is bound to uncover only part of the underreporting as it is likely that

many cases never come to the attention of either physician or insurer. Our model shows underreporting by a factor of about three. Our factor is smaller than the factor ten of [21], but it is still an affirmation that the problem is significantly bigger than it appears from official numbers.

Sero-epidemiological surveys [39,40] suggest that there are essentially no susceptible adolescents and adults in the orthodox Protestant community, i.e., all susceptibles are infected before they reach their late teenage years. The survey results, however, are hard to reconcile with the numbers shown in Table 1. Table 1 shows a significant number of adolescent and adult cases and also a substantial increase in adolescent and adult cases from the 1999/2000 to the 2013/2014 outbreak. The original Kermack-McKendrick model already describes how, in any epidemic, there is always a fraction of susceptibles that does not get infected. For our system, an ever increasing number of adult susceptibles since 1977 is the result. The enhanced model in Section 4.2 expands on this result. The results of the enhanced model are consistent with the data in Table 1 and tell us that the increase of adolescent and adult cases from one outbreak to the next is a trend that is likely to continue. The trend is worrisome as the measles provokes more serious symptoms when it strikes an adolescent or adult as compared to a child – complications are more likely and hospitalization is more often necessary. More susceptible adults and adolescents results in a higher burden on the public health system.

We are grateful to the Rijksinstituut voor Volksgezondheid en Milieu (the Dutch National Institute for Public Health and the Environment) for providing us with graphics and allowing us to use them. Both authors contributed equally to this paper.

References

1. P.M. Strebel, S.L. Cochi, E. Hoekstra, P.A. Rota, D. Featherstone, W.J. Bellini, S.L. Katz, *J. Infect. Dis.* **204**, S1 (2011)
2. R.T. Perry, M. Gacic-Dobo, A. Dabagh, M.N. Mulders, P.M. Strebel, J.M. Okwo-Bele, P.A. Rota, J.L. Goodson, *Morb. Mortal. Wkly. Rep.* **63**, 103 (2014)
3. I. Steffens, R. Martin, P.L. Lopalco, *Euro Surveill.* **15**, 19749 (2010)
4. E.A. van Lier, P.J. Oomen, M. Mulder, M.A.E. Conyn-van Spaendonck, I.H. Drijfhout, P.A.A.M. de Hoogh, H.E. de Melker, Dutch National Institute for Public Health and the Environment (RIVM) report 150202001/2013 (2013), <http://www.rivm.nl/bibliotheek/rapporten/150202001.pdf>
5. W.L. Ruijs, J.L. Hautvast, G. van IJzendoorn, W.J. van Ansem, G. Elwyn, K. van der Velden, M.E. Hulscher, *BMC Health Serv. Res.* **12**, 231 (2012)
6. W.L. Ruijs, J. van Klinken, *Vaccinatie in de reformatische gezindte – Informatie voor de jeugdgezondheidszorg*, Dutch National Institute for Public Health and the Environment (RIVM), Brochure (2013), http://www.npvzorg.nl/fileadmin/user_upload/documents/Vaccinatie/Brochure-professionals_spreads.pdf

7. W.L. Ruijs, J.L. Hautvast, S. Kerrar, K. van der Velden, M.E. Hulscher, *BMC Public Health* **13**, 511 (2013)
8. W.L. Ruijs, J.L. Hautvast, W.J. van Ansem, R.P. Akkermans, K. van 't Spijker, M.E. Hulscher, K. van der Velden, *Eur. J. Public Health* **22**, 359 (2012)
9. W.H. McNeill, *Plagues and Peoples* (Anchor Books, New York, 1976)
10. P.L. Panum, *Observations Made During the Epidemic of Measles on the Faroe Islands in the Year 1846 (a translation from the Danish)* (Delta Omega Society, New York, 1940), <http://www.deltaomega.org/documents/PanumFaroeIslands.pdf>
11. L. Edelstein-Keshet, *Mathematical Models in Biology* (SIAM, Philadelphia, 1988)
12. C.C. Wielders, R.S. Van Binnendijk, B.E. Snijders, G.A. Tipples, J. Cremer, E. Fanoy, S. Dolman, W.L. Ruijs, H.J. Boot, H.E. de Melker, S.J. Hahné, *Euro Surveill.* **16**, 19989 (2011)
13. N.J. Gay, *J. Infect. Dis.* **189**, S27 (2004)
14. M. van Boven, M. Kretzschmar, J. Wallinga, P.D. O'Neill, O. Wichmann, S. Hahné, *J. R. Soc. Interface* **7**, 1537 (2010)
15. A. van Ginkel, S. Hahné, Dutch National Institute for Public Health and the Environment (RIVM), Mazelen surveillance overzicht, 1 mei 2013–12 feb 2014 (2014), <http://www.rivm.nl/dsresource?objectid=rivmp:210291&type=org&disposition=inline>
16. O. Wichmann, A. Siedler, D. Sagebiel, W. Hellenbrand, S. Santibanez, A. Mankertz, G. Vogt, U. van Treeck, G. Krause, *Bull. World Health Organ.* **87**, 108 (2009)
17. M.J. Knol, A.T. Urbanus, E.M. Swart, L. Mollema, W.L. Ruijs, R.S. van Binnendijk, M.J. te Wierik, H.E. de Melker, A. Timen, S.J. Hahné, *Euro Surveill.* **18**, 20580 (2013)
18. J. Wallinga, J.C. Heijne, M. Kretzschmar, *PLOS Med.* **2**, e316 (2005)
19. W.O. Kermack, A.G. McKendrick, *Proc. Roy. Soc. A* **115**, 700 (1927) [Reprinted in *Bull. Math. Biol.* **53**, 33 (1991)]
20. J.D. Murray, *Mathematical Biology*, 2nd Corrected edn. (Springer-Verlag, New York, 1993)
21. C.E.D. van Isterdael, G.A. van Essen, M.M. Kuyvenhoven, A.W. Hoes, W.A.B. Stalman, N.J. de Wit, *J. Clin. Epidemiol.* **57**, 633 (2004)
22. A. Mette, A.M. Reuss, M. Feig, L. Kappelmayer, A. Siedler, T. Eckmanns, G. Poggensee, *Dtsch. Arztebl. Int.* **108**, 191 (2011)
23. C. Six, J. Blanes de Canecaude, J.L. Duponchel, E. Lafont, A. Decoppet, M. Travanut, J.M. Pingeon, L. Coulon, F. Peloux-Petiot, P. Grenier-Tisserant, J.C. Delarozière, F. Charlet, P. Malfait, *Euro Surveill.* **15**, 19754 (2010)
24. J.A. Yorke, W.P. London, *Am. J. Epidemiol.* **98**, 453 (1973)
25. M.J. Keeling, P. Rohani, *Modeling Infectious Diseases in Humans and Animals* (Princeton University Press, New Jersey, 2008)
26. L.F. Olsen, W.M. Schaffer, *Science* **249**, 499 (1990)
27. L. Stone, R. Olinky, A. Huppert, *Nature* **446**, 533 (2007)
28. B.M. Bolker, B.T. Grenfell, *Proc. Natl. Acad. Sci. USA* **93**, 12648 (1996)
29. H.B. Fortuin, Dutch National Institute for Public Health and the Environment (RIVM), *Infectieziekten Bulletin* **4**, 1 (1993), <http://rivm.nl/dsresource?type=pdf&objectid=rivmp:47245&versionid=&subjectname=>
30. E. van Velzen, E. de Coster, R. van Binnendijk, S. Hahné, *Euro Surveill.* **13**, 18945 (2008)
31. S. Hahné, M. te Wierik, L. Mollema, E. van Velzen, E. de Coster, C. Swaan, H. de Melker, R. van Binnendijk, *Emerg. Infect. Dis.* **16**, 567 (2010)
32. M. Muscat, *J. Infect. Dis.* **204**, S353 (2011)
33. I.A. Harmsen, R.A.C. Ruiter, T.G.W. Paulussen, L. Mollema, G. Kok, H.E. de Melker, *Adv. Prev. Med.* **2012**, 175694 (2012)
34. S.L.N. Zwakhals, E.A. van Lier, H. Giesbers, Dutch National Institute for Public Health and the Environment (RIVM), Vestigingen antroposofisch scholen 2012 in *Volksgezondheid Toekomst Verkenning, Nationale Atlas Volksgezondheid*, Bilthoven, 2012, <http://www.zorgatlas.nl/preventie/vaccinaties-en-screening/vestigingen-antroposofisch-scholen-2012/>
35. D. Mollison, *Math. Biosci.* **107**, 255 (1991)
36. N.G. Van Kampen, *Stochastic Processes in Physics and Chemistry* (Elsevier, Amsterdam, 1992)
37. M.I. Dykman, I.B. Schwartz, A.S. Landman, *Phys. Rev. Lett.* **101**, 078101 (2008)
38. M. Khasin, M.I. Dykman, B. Meerson, *Phys. Rev. E* **81**, 051925 (2010)
39. S. van den Hof, G.A.M. Berbers, H.E. Melker, M.A.E. Conyn-van Spaendonck, *Vaccine* **18**, 931 (2000)
40. L. Mollema, G.P. Smits, G.A. Berbers, F.R. van der Klis, R.S. Binnendijk, H.E. Melker, S.J.M. Hahné, *Epidemiol. Infect.* **142**, 1100 (2014)
41. H. Bijkerk, M.A.J. Bilkert-Mooiman, H.J. Houtters, *Nederlands Tijdschrift voor Geneeskunde* **133**, 29 (1989)
42. S. van den Hof, M.A. Conyn-van Spaendonck, J.E. van Steenberghe, *J. Infect. Dis.* **186**, 1483 (2002)

Open Access This is an open access article distributed under the terms of the Creative Commons Attribution License (<http://creativecommons.org/licenses/by/4.0>), which permits unrestricted use, distribution, and reproduction in any medium, provided the original work is properly cited.